

Cellular automata in the light of COVID-19

Sourav Chowdhury* Suparna Roychowdhury† Indranath Chaudhuri‡

Department of Physics, St. Xavier's College (Autonomous)
30 Mother Teresa Sarani, Kolkata-700016, West Bengal, India

August 1, 2023

Abstract

Currently, the world has been facing the brunt of a pandemic due to a diseases called COVID-19 for the last two years. To study the spread of such infectious diseases it is important to not only understand their temporal evolution but also the spatial evolution. In this work, the spread of this disease has been studied with a cellular automata (CA) model to find the temporal and the spatial behavior of it. Here, we have proposed a neighborhood criteria which will help us to measure the social confinement at the time of the disease spread. The two main parameters of our model are (i) disease transmission probability (q) which helps us to measure the infectivity of a disease and (ii) exponent (n) which helps us to measure the degree of the social confinement. Here, we have studied various spatial growths of the disease by simulating this CA model. Finally we have tried to fit our model with the COVID-19 data of India for various waves and have attempted to match our model predictions with regards to each wave to see how the different parameters vary with respect to infectivity and restrictions in social interaction.

Introduction

Epidemics and pandemics have a long story throughout human history. Recently human civilization has faced another pandemic named COVID-19. This pandemic has affected many countries through multiple waves. Total of 504,451,689 people have been infected worldwide and 6,222,430 people have died due to COVID-19 till 17 April 2022. In India 43,042,097 people have suffered and 521,781 have died as of 17/04/2022 due to this disease.¹ COVID-19 is caused by the virus which is named SARS COV-2. Multiple variants of this virus, like delta, omicron and many others makes it harder to control and predict its behavior. Recently another variant of COVID-19 named XE has been found.² Mathematical modeling helps us to understand the behavior of disease spread such that prevention and control strategies can be built. Also, mathematical models can help us to find some inherent properties of the disease and nature of its spread.

There are many different types of models that have been used in the past to study various diseases. These models are mainly modified versions of the Kermack McKendrick SIR model which is based on a system of coupled ordinary differential equations.³ Currently, the ODE-based models and statistical models are widely used in literature to model the temporal behavior of the spread of COVID-19 from different aspects. Most of these models have tried to analyze the spread of this disease and tried to predict its future behavior.⁴⁻⁷ There are models which have proposed various intervention and vaccination strategies to prevent and control the spread of the disease.⁸⁻¹² Also, some authors have tried to predict different inherent properties of this pandemic like herd immunity and its chaotic nature.¹³⁻¹⁷ These temporal models can give us much valuable information, however most of these models assume that a population is homogeneously mixed and cannot describe any spatial behavior. To incorporate this spatial behavior, deterministic and probabilistic Spatio-temporal models have been used in recent studies. Cellular automata (CA) is one such kind of spatio-temporal model.

Cellular automata (CA) has been used in many studies to model different aspects of epidemics. It has been widely used to model the disease spread of influenza and various vector-borne diseases like dengue.¹⁸⁻²⁶ A neighborhood condition is an important aspect in the CA. The most used neighborhood conditions are (i) Neumann's neighborhood condition, (ii) Moore's neighborhood condition, (iii) Extended neighborhood condition, and (iv) Random interactions. Coupled with these neighborhood conditions, various models like SEIR, SEIRS, SEIRD, and SEIRQD have been studied with the help of CA to model the spatial growth of epidemics.^{19,22,27-32} Currently, CA has gained a lot of momentum in the studies of COVID-19. Various advanced studies with Genetic algorithms and network models have been for COVID-19 data.³³⁻³⁸ Also there are models where COVID-19 has studied from different aspects.

In this paper, we have tried to model COVID-19 using cellular automata (CA) to find spatio-temporal behavior of it. We have also made some analysis to understand its behavior in different waves of the disease. A cellular automata (CA) model

*email: chowdhury95sourav@gmail.com

†email: suparna@sxccal.edu

‡email: indranath@sxccal.edu

is represented in a square lattice and defined by some neighborhood and boundary conditions, the details of which are given in following sections.

This paper is arranged as follows: Section 2 consists of a detailed discussion of the model, neighborhood conditions, probability of infection, and the algorithm of the model. The result of the simulation has been shown in section 3 and the data analysis is shown in section 4. Finally, Section 5 consists of the conclusions of our model.

2 Mathematical Model

In this article, we have illustrated a Cellular automata (CA) model for epidemics and assumed the SEIR model as the base model. SEIR model stands for Susceptible-Exposed-Infectious-Removed. Here we have considered a $N \times N$ square lattice, where each cell of the lattice is assumed to be a person. Each cell of the lattice can have the set of states, $\mathcal{S} = \{S, E, I, R\}$ and these states are represented by the values $\mathcal{V} = \{0, 1, 2, 3\}$. The updation of a cell's state depends upon various conditions like, (i) the current state of the cell, (ii) the amount of time spent in the current state, and (iii) the current states of the neighbors. The main assumptions of our model are given below:

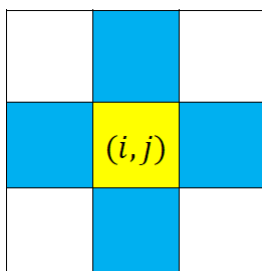
- Every cell represents a person.
- Only susceptible persons can interact with the other cells.
- A removed person cannot be infected again.
- For this CA model, we have assumed a periodic boundary condition. If a cell of i th row and j th column of a $N \times N$ lattice is denoted by (i, j) then,

$$\begin{aligned} (N + 1, j) &\equiv (1, j) & j = 0, 1, \dots, N. \\ (i, N + 1) &\equiv (i, 1) & i = 0, 1, \dots, N. \end{aligned} \quad (1)$$

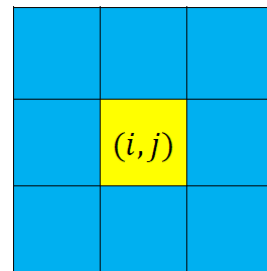
- One susceptible person can interact with a single person in each time step.

2.1 Neighborhood condition

Nearest neighborhood condition is a widely used concept in the literature. Here, it has been assumed that a particular cell can only interact with its nearest neighborhood cells. Such two famous neighborhood conditions are: (i) Neumann's neighborhood condition and (ii) Moore's neighborhood condition.



(a) Neumann's neighborhood condition.



(b) Moore's neighborhood condition.

Figure 1: Different neighborhood conditions. Blue cells represent the nearest neighborhoods of (i, j) cell.

Fig. 1 shows the two neighborhood conditions. Fig. 1a shows Neumann's neighborhood condition, where the nearest neighborhoods of any chosen (i, j) cell are the first neighborhood cells with respect to the chosen cell. Similarly, Fig. 1b shows Moore's neighborhood condition. In this case, all first and second neighborhoods are treated as the nearest neighborhoods of the chosen (i, j) cell.

In this work, we have assumed that a cell can interact with any other cells depending on the probability of interaction (p_{int}) between them. Here we have assumed that the probability of interaction (p_{int}) of a cell (i, j) to any other cell varies inversely as a function of d (distance between two cells) in the form of a power law. Hence,

$$p_{int}(d) \propto \frac{1}{d^n} \quad (2)$$

where n is the degree exponent and can have a value greater than zero. Here, we have assumed that the distance between two cells is not just the geometrical distance between two. It depends on the layer number (l). In Fig. 2, we have shown how

layers are defined. Also, it shows that a layer l contains the $8l$ number of cells. If we choose a lattice of size $N \times N$ then the total number of layers in this lattice is $L = \frac{N-1}{2}$, when N is odd.

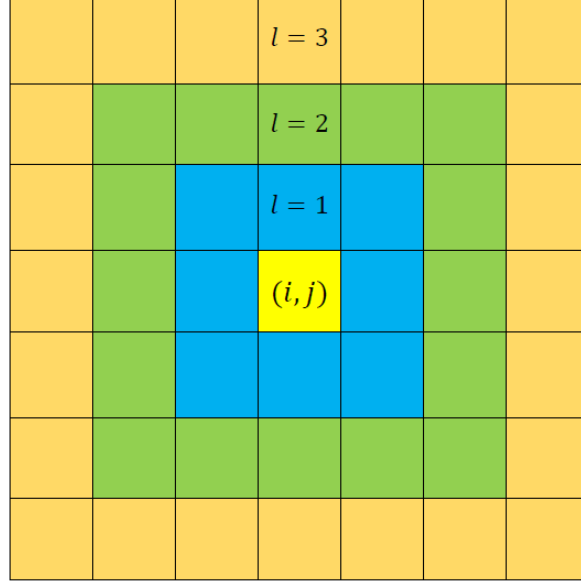


Figure 2: Different layers of a lattice with respect to (i, j) cell.

Hence, we can write,

$$d \propto l. \quad (3)$$

For mathematical simplicity, we can assume $d = l$. Hence, from Eq. 2 we can write,

$$p_{int}(d) = p_{int}(l) \propto \frac{1}{l^n} \quad (4)$$

If there are L number of layers then the above equation can be written as,

$$p_{int}(l) = \frac{\frac{1}{l^n}}{\sum_{l=1}^L \frac{1}{l^n}} = \frac{1}{A_n l^n} \quad (5)$$

where, $A_n = \sum_{l=1}^L \frac{1}{l^n}$. Hence, a person at the (i, j) cell can interact with any other cell of layer l with a probability $p_{int}(l)$. Thus, average interaction distance ($\langle d \rangle$) can be defined as,

$$\langle d \rangle = \sum_{l=1}^L l p_{int}(l) = \frac{1}{A_n} \sum_{l=1}^L l \frac{1}{l^n} = \frac{1}{A_n} \sum_{l=1}^L \frac{1}{l^{n-1}} \quad (6)$$

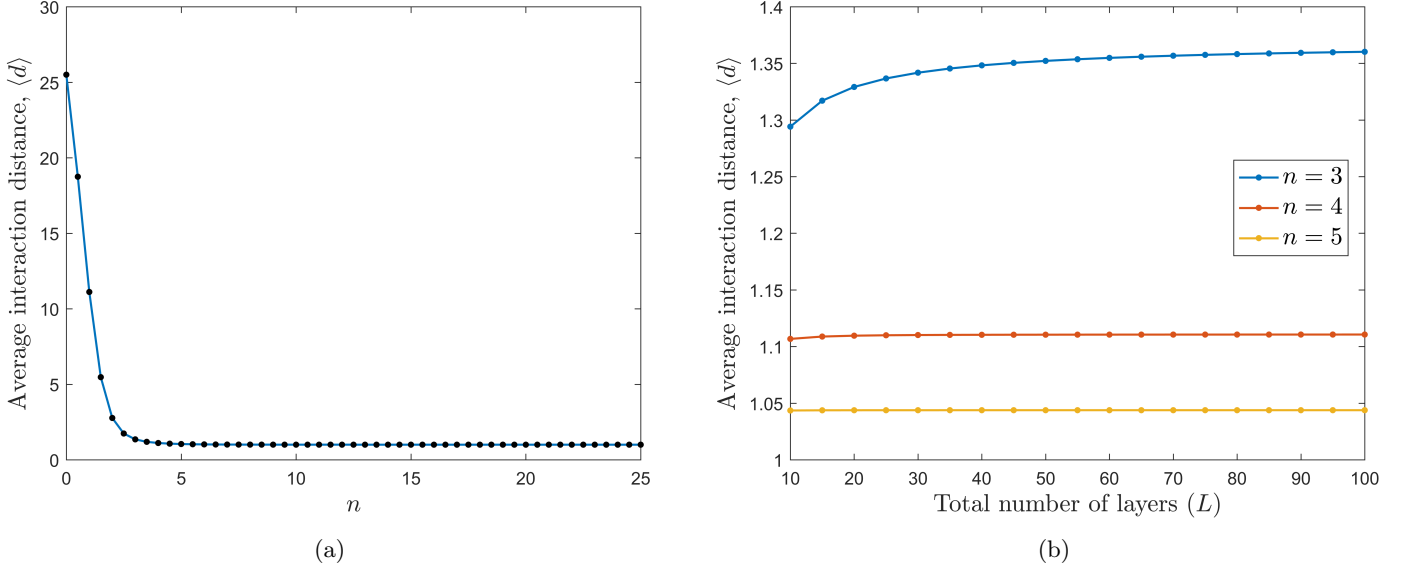


Figure 3: Plots of average interaction distance ($\langle d \rangle$) with n and the total number of layers (L). (a) Plot of average interaction distance ($\langle d \rangle$) with n by considering the total number of layers (L) = 50. (b) Plot of average interaction distance ($\langle d \rangle$) with the total number of layers (L) for $n=3,4$, and 5.

Fig. 3a shows the variation of average interaction distance ($\langle d \rangle$) with the degree exponent (n). From this figure, it can be found that the average interaction distance ($\langle d \rangle$) is quickly decreases and saturates to unity as n increases. Also, from Fig. 3b it can be seen that the average interaction distance ($\langle d \rangle$) is approximately ~ 1 for exponents $n > 3$. Hence for $n \gg 3$ the neighborhood condition is approximately similar to Moore's neighborhood condition as discussed earlier and does not give any significantly different results.

2.2 Probability of infection (Q_I)

Let, q denote the disease transmission probability when a susceptible and an infectious person interact. The probability that a susceptible person will interact with any person at the layer l is $p_{int}(l)$. If the probability of finding an infectious person in that layer is $p_I(l)$ then the probability that the susceptible person will be infected is $qp_{int}(l)p_I(l)$. Hence, the probability of infection (Q_I) of a susceptible person is,

$$Q_I = q \sum_{l=1}^L p_{int}(l)p_I(l). \quad (7)$$

As, $p_{int}(l) = \frac{1}{A_n l^n}$, from the above equation (Eq. 7) we can write,

$$Q_I = \frac{q}{A_n} \sum_{l=1}^L \frac{p_I(l)}{l^n} \quad (8)$$

From the above equation (Eq. 8) we can say that the terms with small layer number (l) dominate the summation. Hence, the infection possibility of a susceptible person mainly depends on the infection situation around the person.

Thus in our model, instead of choosing a traditional neighborhood condition where the degree of the interaction is fixed, we have assumed a model where we can vary the degree of the social confinement by changing n (degree exponent). Also we have calculated the probability of infection (Q_I) for this modified model.

3 Algorithm and Simulations

3.1 Algorithm

Here, we have discussed the state updation algorithm of the SEIR model. As we have mentioned earlier, every cell's state is denoted by a value (v) which is present in this set $\{0, 1, 2, 3\}$. The algorithm is given below:

- Let, at time t there is a susceptible person at (i, j) cell. So, the value of the (i, j) cell is $v(i, j, t) = 0$ and the probability of infection is $Q_I(i, j, t)$. To find the infection possibility of the susceptible person, we will generate a uniform random number u between 0 and 1.

If, $u \leq Q_I(i, j, t)$ then the susceptible person is exposed and at time $t + 1$ the state of the (i, j) cell will be changed from $v = 0$ to $v = 1$.

else, at time $t + 1$ the state of the (i, j) cell will be unchanged.

- An exposed person ($v = 1$) will remain exposed for τ_I number of days. After that, the person will be infectious and the state of the corresponding cell will be changed from $v = 1$ to $v = 2$.
- An infectious person will remain in this state for τ_R number of days. After that, the person will be removed (recovered or dead) and the state of the cell will be changed from $v = 2$ to $v = 3$.

3.2 Simulation

In this part, we have done simulation of our model with $n = 1, 2, 3$. The values of the parameters and initial conditions that are used in the simulations are listed in the tables (Table 1 and Table 2) below:

Description of the parameters	Parameters	Values of the parameters
Lattice size	$N \times N$	101×101
Disease transmission probability	q	0.3
Latency period of the disease	τ_I	8 days
Removal period	τ_R	18 days

Table 1: Table for the parameter values that are used in the simulations.

States	Initial values
$S(0)$	10200
$I(0)$	1
$E(0)$	0
$R(0)$	0

Table 2: Table for the initial conditions of the simulations.

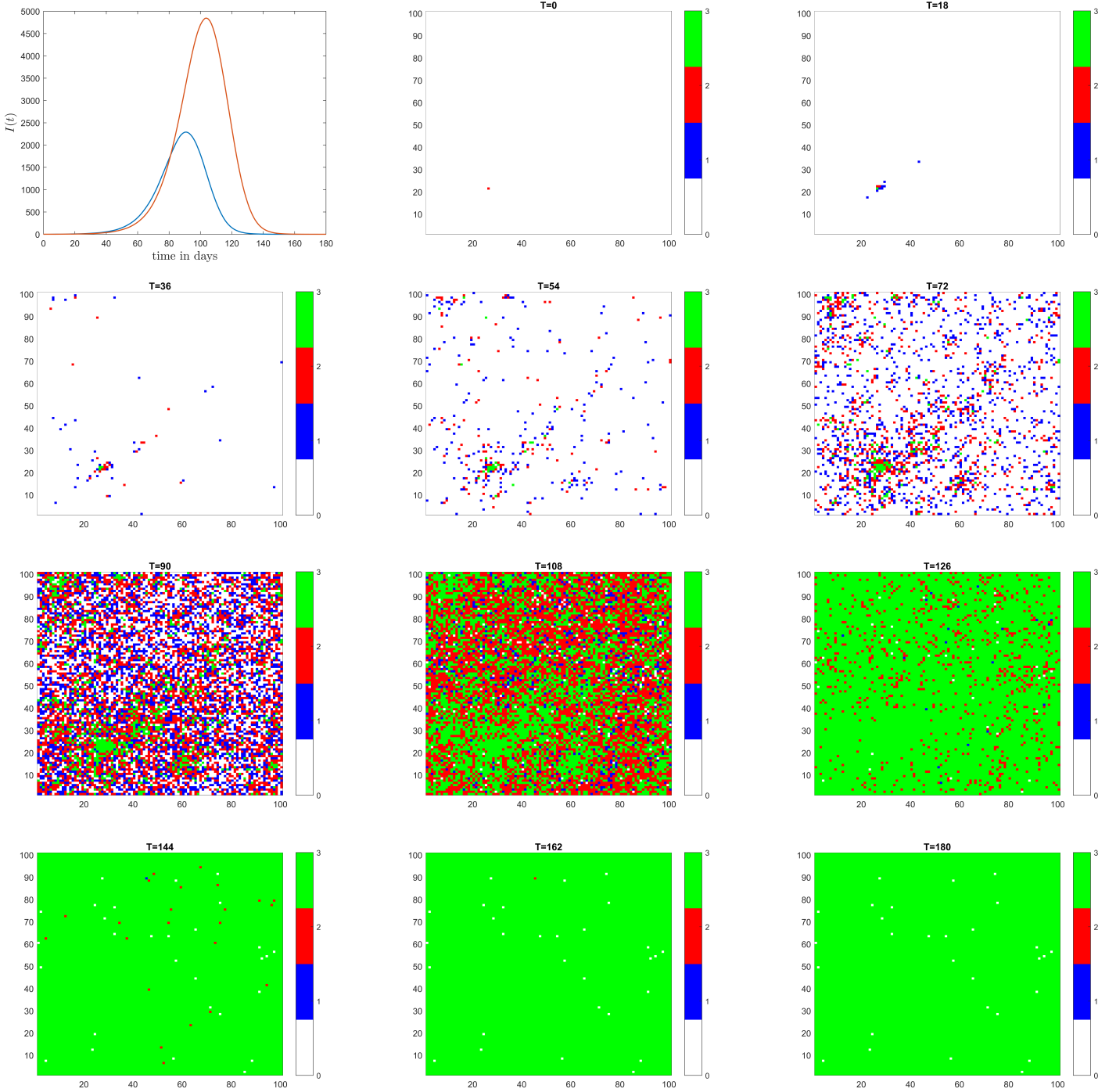


Figure 4: Plots of the temporal and spatial behavior of the disease spread for $n = 1$.

In Fig. 4, the first plot shows the temporal behavior of the exposed cases ($E(t)$) and the infectious cases ($I(t)$) of the epidemic. These temporal plots are averaged on 50 simulation samples. The rest plots of Fig. 4 are CA plots that represent the spatial evolution of disease spread. From these CA plots, we can hardly detect any clustering of the infected cases. This happens because the average interaction distance, $\langle d \rangle \approx 11.11$. Thus a susceptible person can be infected by an infectious person who is far away from the susceptible one.

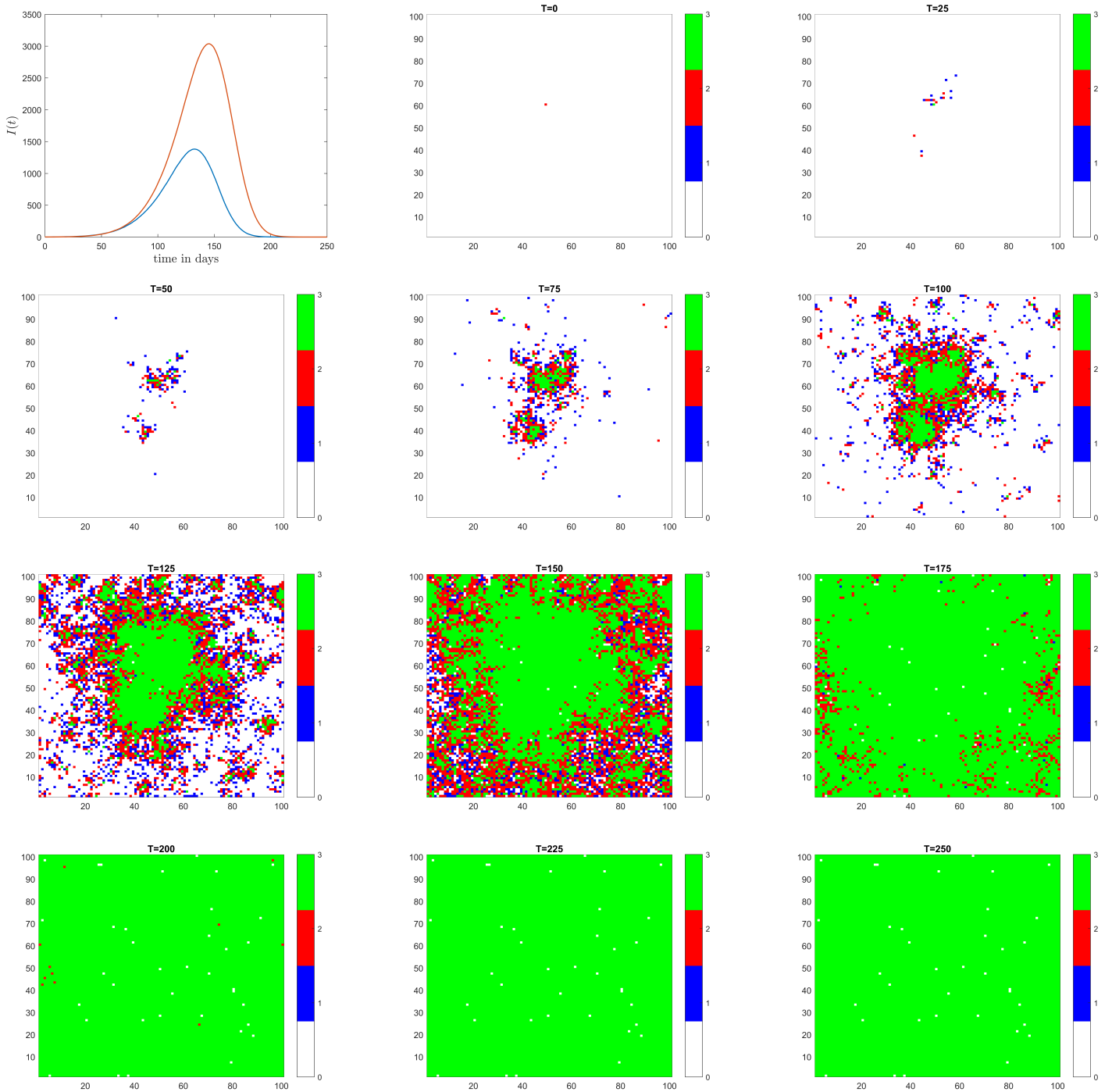


Figure 5: Plots of the temporal and spatial behavior of the disease spread for $n = 2$.

In Fig. 5, the first plot again shows the temporal growth of the epidemic. It can be seen from the CA plots that for $n = 2$, clusters are formed. The reason behind this is the short average interaction distance. For $n = 2$, the average interaction distance, $\langle d \rangle \approx 2.77$. Also from the temporal plot, we can see that the infection spread time is increased than in the $n = 1$ case. This is also because of the short average interaction distance. For a short average interaction distance, only a few susceptible persons can interact with the infectious person. So, if most of those susceptible persons become infected then the infectious person cannot spread the disease further. Whereas, for $n = 1$ case, an infectious person can interact with many susceptible persons. Hence, an infectious person can infect more people during the infectious period.

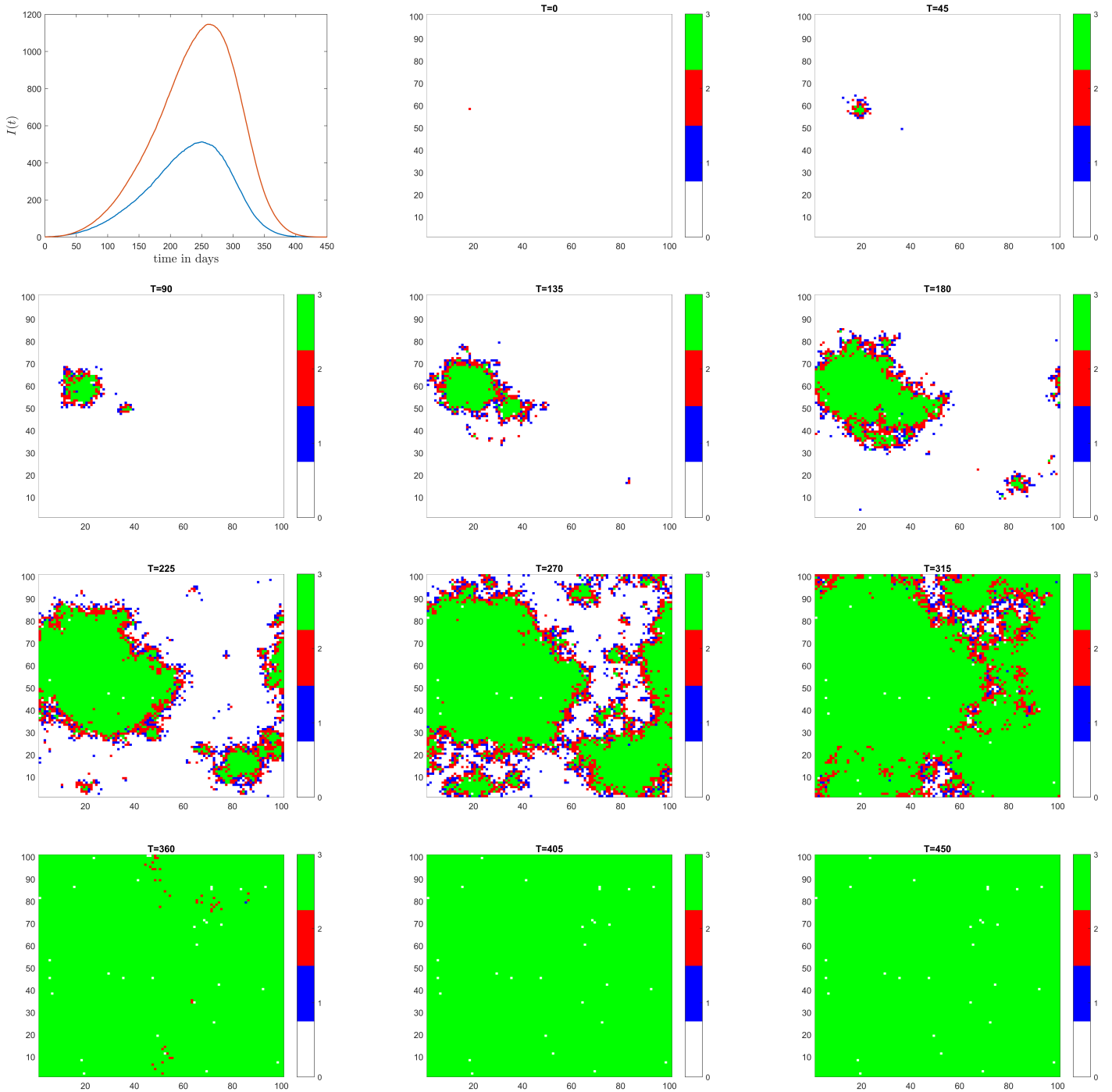


Figure 6: Plots of the temporal and spatial behavior of the disease spread for $n = 3$.

Fig. 6 shows the evolution of the disease for $n = 3$. Here we can also clearly find the clusters. These clusters are more prominent than the $n = 2$ case because of the less average interaction distance ($\langle d \rangle$). Value of the average interaction distance for $n = 3$ is $\langle d \rangle \approx 1.35$. Here we can see that the disease takes a longer time to fall for $n = 3$ than for $n = 1$ and $n = 2$. The reason behind this is the lower value of the average interaction distance which is discussed earlier.

Hence, from the above discussions, we can conclude that the clustering behavior of the disease spread depends on the average interaction distance ($\langle d \rangle$) as well as on degree exponent n . Also, the average interaction distance ($\langle d \rangle$), gives an average estimation of the number of susceptible persons who can interact with an infectious person which is represented by $8\langle d \rangle$. So, for a large $\langle d \rangle$ (or small n) an infectious person can spread the disease to distanced region. Thus the infection period depends on the average interaction distance ($\langle d \rangle$) and also on n .

4 Comparison with data

In this section, we have tried to fit our model with current COVID-19 data. Our model has four free parameters which are, (i) q : disease transmission probability, (ii) n : degree exponent, (iii) τ_I : mean latency period, (iv) τ_R : mean infectious period. We have optimized these free parameters for different waves of the COVID-19 pandemic in India. Here, we have considered each wave separately and normalized the active cases of each wave with the total number of infected cases in the respective wave. The data is taken from covid19india.org.³⁹ The date range of the different waves that we have considered here are given below:

Waves	Start date	End date
First wave	30-Jan-2020	16-Feb-2021
Second wave	17-Feb-2021	31-Oct-2021

Table 3: Date ranges for different waves.

To fit the model with the data we have optimized the sum of squared errors (SSE)

$$SSE = \sum_k (i_k^d - i_k)^2 \quad (9)$$

i_k^d : fraction of the active cases from the data. i_k : fraction of the infectious cases from the model.
The results of the best fit parameter values are given below.

Waves	q	n	τ_I (days)	τ_R (days)
First wave	0.1950	1.9310	5	11
Second wave	0.2406	1.3449	8	10

Table 4: Fitting parameter values for different waves.

We have optimized COVID-19 data with a 101×101 lattice space. Fig 7a and 7b shows the fitted model along with data for the first and the second wave.

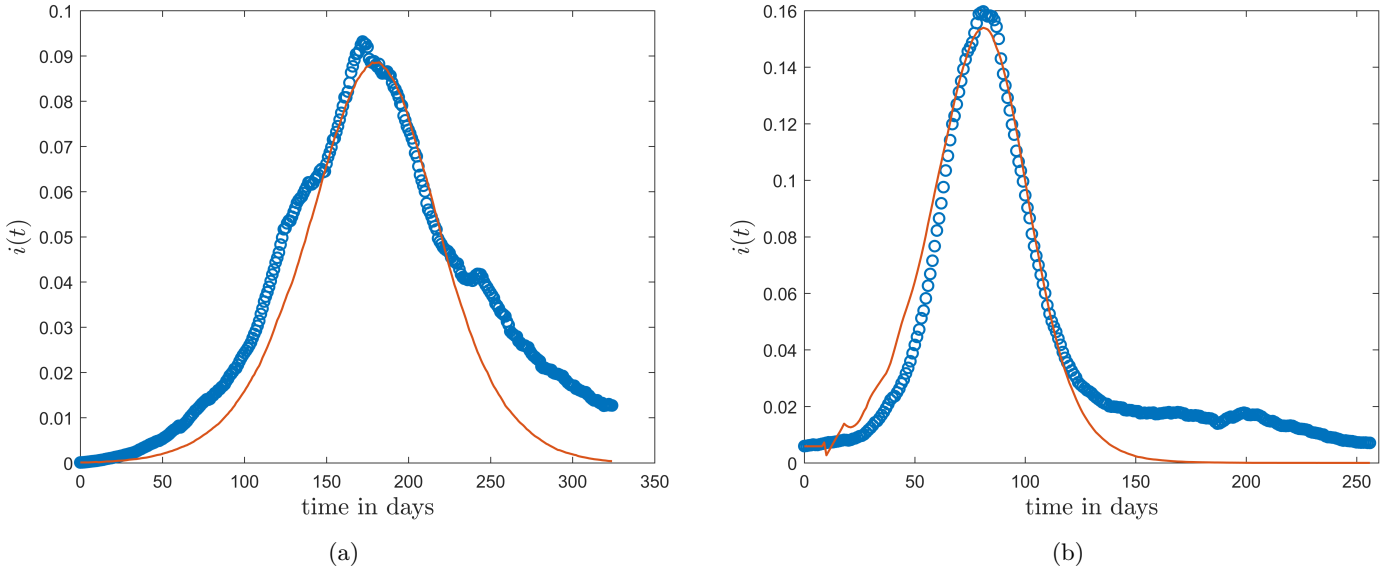


Figure 7: Model fitting of the COVID-19 data of India (a) Model fitting of the first wave. (b) Model fitting of the second wave.

Here we can see that the model fits reasonably well with the data. Also from the table 4, we see that the disease transmission probability (q) increases and the degree exponent (n) decreases in the second wave as compared to the first wave. Increment of q represents that in the second wave of the disease it was possibly more infectious and spread faster than in the first wave. Also decrement of n indicates that the interaction between infectious and the susceptible population spread out to a larger distances in the second wave as compared to the first wave. This is possibly because of the COVID protocols which is relaxed much more in the initial phase of the second wave as compared to the first wave.

5 Conclusions

In this section we have summarized the main features and results of our model. The cellular automata (CA) is a very common tool to model a disease spread and has been used extensively in literature for studying different systems. In this paper, we have modeled the CA by proposing a new neighborhood criteria. Usually in earlier studies, neighborhood condition is such that the neighborhood of a lattice cell is always fixed. Whereas in our model, rather than choosing a specific neighborhood condition, we assume that a lattice cell can interact with any other cell at distance d with a certain probability which is called interaction probability ($p_{int}(d)$) (Eq.5). We have assumed that the interaction probability ($p_{int}(d)$) is a function of the distance (d) and has a form of inverse power law with degree exponent n . Here, exponent n is a very important parameter as it enables us to tune the social confinement of our model. With this newly defined neighborhood criteria, we have calculated various relations like average interaction distance ($\langle d \rangle$) and the probability of infection (Q_I) to understand and represent our model properly.

From Fig. 3a, we can see that the average interaction distance ($\langle d \rangle$) decreases and saturation is reached to ~ 1 as n increases. So, for a higher n , a person can mainly interact with nearest neighbors. However, for a smaller value of n , a person can interact with the distant neighbors. Hence higher values of n represents higher social confinement and vice-versa. Also we want to mention that for exponents, $n > 3$, the average interaction distance, $\langle d \rangle \approx 1$. Thus the values $n \gg 3$ do not give us any new results.

In the simulation section, we have studied the temporal and spatial behavior of our model for different degree exponents (n). As n increases, the disease spread becomes slower and it is more clustered. This happens because of the decrease in the average interaction distance ($\langle d \rangle$) or in the other words increase in the social confinement with increasing values of n . Thus the disease transmission probability (q) and the degree exponent n regulates the speed of the disease spread.

Also, we have compared our model with COVID-19 data of India for different waves. We have first normalized the active cases of a wave with the total number of infected cases in that wave. Then we have optimized the sum of squared errors of the infectious cases (Eq. 9) to get the best fit result with the data. Here all simulations are done on a 101×101 lattice. We have found that the disease transmission probability (q) increases in the second wave than the first wave. This means that the disease is more infectious in the second wave than the first wave. Also the degree exponent (n) decreases in the second wave. This implies that the decrement in the COVID-19 restrictions (or decrement in the degree of social confinement) at the initial time of the second wave played a significant role to the faster spread of the disease. Our model fits the peak of the waves well, however fall in the data at the end of both waves and plateauing at the end of the second wave has some matches with our fitted model. This possibly indicates that our model needs to be modified to incorporate these aspects which we will look at in our future works.

Modeling spread of a disease is a very complicated process since several factors have to be considered. Non-uniform distribution of the population and economic situation of the regions are two major factors which affects the disease spread. In future we want to look at these complex aspects by refining this model to find the behavior of the disease spreading more accurately. We would also like to study these possibilities in the context of COVID-19.

Acknowledgment

The authors would like to thank the Department of Physics, St. Xavier's College, Kolkata for providing support during this work. One of the authors (S. C.) acknowledges the financial support provided from the University Grant Commission (UGC) of the Government of India, in the form of CSIR-UGC NET-JRF. Finally, the authors would also like to express their gratitude to the anonymous referee for his/her valuable comments and suggestions.

References

- [1] *Live update of COVID-19 situation in different countries- Worldometers.* <https://www.worldometers.info/coronavirus/>.
- [2] *Tracking SARS-CoV-2 variants (WHO).* <https://www.who.int/en/activities/tracking-SARS-CoV-2-variants/>.
- [3] William Ogilvy Kermack, A. G. McKendrick, and Gilbert Thomas Walker. A contribution to the mathematical theory of epidemics. *Proceedings of the Royal Society of London. Series A, Containing Papers of a Mathematical and Physical Character*, 115(772):700, 1927. DOI: 10.1098/rspa.1927.0118.
- [4] Supriya Mondal and Sabyasachi Ghosh. Mapping first to second wave transition of covid19 indian data via sigmoid function and prediction of third wave. *medRxiv*, 2021. DOI: 10.1101/2021.07.11.21260325.
- [5] Sandip Mandal, Nimalan Arinaminpathy, Balram Bhargava, and Samiran Panda. Plausibility of a third wave of covid-19 in india: A mathematical modelling based analysis. *The Indian journal of medical research*, 153(5):522, 2021.

- [6] C Kavitha, A Gowrisankar, and Santo Banerjee. The second and third waves in india: when will the pandemic be culminated? *The European Physical Journal Plus*, 136(5):596, 2021.
- [7] A Gowrisankar, TMC Priyanka, and Santo Banerjee. Omicron: a mysterious variant of concern. *The European Physical Journal Plus*, 137(1):100, 2022.
- [8] Brody H. Foy, Brian Wahl, Kayur Mehta, Anita Shet, Gautam I. Menon, and Carl Britto. Comparing covid-19 vaccine allocation strategies in india: A mathematical modelling study. *International Journal of Infectious Diseases*, 103:431, 2021. DOI: 10.1016/j.ijid.2020.12.075.
- [9] Namrata Soni, Jyoti Bhola, Ashutosh Yadav, Ishita Srivastva, and Utcارش Mathur. A mathematical reflection of covid-19 and vaccination acceptance in india. 8:150, 2021. DOI: 10.21276/apjhs.2021.8.3.27.
- [10] Ting-Yu Lin, Sih-Han Liao, Chao-Chih Lai, Eugenio Paci, and Shao-Yuan Chuang. Effectiveness of non-pharmaceutical interventions and vaccine for containing the spread of covid-19: Three illustrations before and after vaccination periods. *Journal of the Formosan Medical Association*, 120:S46, 2021. DOI: 10.1016/j.jfma.2021.05.015.
- [11] Simon A Rella, Yuliya A Kulikova, Emmanouil T Dermitzakis, and Fyodor A Kondrashov. Rates of sars-cov-2 transmission and vaccination impact the fate of vaccine-resistant strains. *Scientific Reports*, 11(1):15729, 2021. DOI: 10.1038/s41598-021-95025-3.
- [12] Sourav Chowdhury, Suparna Roychowdhury, and Indranath Chaudhuri. A robust prediction from a minimal model of covid-19—can we avoid the third wave? *arXiv preprint arXiv:2112.08794*, 2021.
- [13] Sourav Chowdhury, Suparna Roychowdhury, and Indranath Chaudhuri. Universality and herd immunity threshold: Revisiting the sir model for covid-19. *International Journal of Modern Physics C*, 32(10):2150128, 2021. DOI: 10.1142/S012918312150128X.
- [14] A Gowrisankar, Lamberto Rondoni, and Santo Banerjee. Can india develop herd immunity against covid-19? *The European Physical Journal Plus*, 135(6):526, 2020.
- [15] André F. Steklain, Ahmed Al-Ghamdi, and Euaggelos E. Zotos. Using chaos indicators to determine vaccine influence on epidemic stabilization. *Phys. Rev. E*, 103:032212, Mar 2021. DOI: 10.1103/PhysRevE.103.032212.
- [16] Jorge Duarte, Cristina Januário, Nuno Martins, Jesús Seoane, and Miguel AF Sanjuán. Controlling infectious diseases: the decisive phase effect on a seasonal vaccination strategy. *arXiv preprint arXiv:2102.08284*, 2021.
- [17] D Easwaramoorthy, A Gowrisankar, A Manimaran, S Nandhini, Lamberto Rondoni, and Santo Banerjee. An exploration of fractal-based prognostic model and comparative analysis for second wave of covid-19 diffusion. *Nonlinear Dynamics*, 106(2):1375–1395, 2021.
- [18] M. J Keeling and C. A Gilligan. Bubonic plague: a metapopulation model of a zoonosis. *Proceedings of the Royal Society of London. Series B: Biological Sciences*, 267(1458):2219–2230, 2000. DOI: 10.1098/rspb.2000.1272.
- [19] A. Holko, M. Medrek, Z. Pastuszek, and K. Phusavat. Epidemiological modeling with a population density map-based cellular automata simulation system. *Expert Systems with Applications*, 48:1–8, 2016. DOI: 10.1016/j.eswa.2015.08.018.
- [20] Khaled M Khalil, M Abdel-Aziz, Taymour T Nazmy, and Abdel-Badeeh M Salem. An agent-based modeling for pandemic influenza in egypt. In *Handbook on Decision Making*, volume 33, pages 205–218. Springer, 2012. DOI: 10.1007/978-3-642-25755-1_11.
- [21] Senthil Athithan, Vidya Prasad Shukla, and Sangappa Ramachandra Biradar. Epidemic spread modeling with time variant infective population using pushdown cellular automata. *Journal of Computational Environmental Sciences*, 2014:769064, 2014. DOI: 10.1155/2014/769064.
- [22] Sheng Bin, Gengxin Sun, and Chih-Cheng Chen. Spread of infectious disease modeling and analysis of different factors on spread of infectious disease based on cellular automata. *International Journal of Environmental Research and Public Health*, 16(23), 2019. DOI: 10.3390/ijerph16234683.
- [23] Gerardo Ortigoza, Fred Brauer, and Iris Neri. Modelling and simulating chikungunya spread with an unstructured triangular cellular automata. *Infectious Disease Modelling*, 5:197–220, 2020. DOI: 10.1016/j.idm.2019.12.005.
- [24] Murali Krishna Enduri and Shivakumar Jolad. Dynamics of dengue disease with human and vector mobility. *Spatial and Spatio-temporal Epidemiology*, 25:57–66, 2018. DOI: 10.1016/j.sste.2018.03.001.
- [25] Puspa Eosina, Taufik Djatna, and Helda Khusun. A cellular automata modeling for visualizing and predicting spreading patterns of dengue fever. *TELKOMNIKA*, 14(1):228, 2016. DOI: 10.12928/TELKOMNIKA.v14i1.2404.

- [26] Emily Burkhead and Jane Hawkins. A cellular automata model of ebola virus dynamics. *Physica A: Statistical Mechanics and its Applications*, 438:424–435, 2015. DOI: 10.1016/j.physa.2015.06.049.
- [27] Armin R. Mikler, Sangeeta Venkatachalam, and Kaja Abbas. Modeling infectious diseases using global stochastic cellular automata. *Journal of Biological Systems*, 13(04):421–439, 2005. DOI: 10.1142/S0218339005001604.
- [28] Henrique Fabricio Gagliardi and Domingos Alves. Small-world effect in epidemics using cellular automata. *Mathematical Population Studies*, 17(2):79–90, 2010. DOI: 10.1080/08898481003689486.
- [29] Quan-Xing Liu, Zhen Jin, and Mao-Xing Liu. Spatial organization and evolution period of the epidemic model using cellular automata. *Phys. Rev. E*, 74:031110, 2006. DOI: 10.1103/PhysRevE.74.031110.
- [30] Liu Quan-Xing and Jin Zhen. Cellular automata modelling of SEIRS. *Chinese Physics*, 14(7):1370–1377, 2005. DOI: 10.1088/1009-1963/14/7/018.
- [31] Leonardo López, Germán Burguener, and Leonardo Giovanini. Addressing population heterogeneity and distribution in epidemics models using a cellular automata approach. *BMC research notes*, 7(1):234, 2014. DOI: 10.1186/1756-0500-7-234.
- [32] Senthil Athithan, Vidya Prasad Shukla, and Sangappa Ramachandra Biradar. Dynamic cellular automata based epidemic spread model for population in patches with movement. *Journal of Computational Environmental Sciences*, 2014:518053, 2014. DOI: 10.1155/2014/518053.
- [33] P.H.T. Schimit. A model based on cellular automata to estimate the social isolation impact on covid-19 spreading in brazil. *Computer Methods and Programs in Biomedicine*, 200:105832, 2021. DOI: 10.1016/j.cmpb.2020.105832.
- [34] P.K. Jithesh. A model based on cellular automata for investigating the impact of lockdown, migration and vaccination on covid-19 dynamics. *Computer Methods and Programs in Biomedicine*, 211:106402, 2021. DOI: 10.1016/j.cmpb.2021.106402.
- [35] Sayantari Ghosh and Saumik Bhattacharya. A data-driven understanding of covid-19 dynamics using sequential genetic algorithm based probabilistic cellular automata. *Applied Soft Computing*, 96:106692, 2020. DOI: 10.1016/j.asoc.2020.106692.
- [36] Larissa M. Fraga, Gina M. B. de Oliveira, and Luiz G. A. Martins. Multistage evolutionary strategies for adjusting a cellular automata-based epidemiological model. In *2021 IEEE Congress on Evolutionary Computation (CEC)*, pages 466–473, 2021. DOI: 10.1109/CEC45853.2021.9504738.
- [37] L. L. Lima and A. P. F. Atman. Impact of mobility restriction in covid-19 superspreading events using agent-based model. *PLOS ONE*, 16(3):1–17, 03 2021. DOI: 10.1371/journal.pone.0248708.
- [38] Anand Sahasranaman and Henrik Jelldoft Jensen. Spread of covid-19 in urban neighbourhoods and slums of the developing world. *Journal of The Royal Society Interface*, 18(174):20200599, 2021. DOI: 10.1098/rsif.2020.0599.
- [39] *COVID-19 data source*. <https://www.covid19india.org/>.